

## The Production of NO/NO<sub>2</sub> Emissions In Propane-Syngas Mixture Diffusion Flame

Bouhental B.<sup>1,2,\*</sup>, Hedef A.<sup>3</sup>, Aouachria Z. and Mameri A.<sup>3</sup>

<sup>1</sup> Department of Materials Science, University of Batna 1, Batna 05000, Algeria

<sup>2</sup> Applied Energy Physics Laboratory (LPEA), Univ. Batna1, 05000 Algeria

<sup>3</sup> CMASMTF Laboratory Department of Mechanical Engineering, FSSA, University Oum El Bouaghi, Algeria

\* (bigaud.bouhental@univ-batna.dz) Email of the corresponding author

Received: 03 July 2023, Accepted: 24 July 2023)

(5th International Conference on Applied Engineering and Natural Sciences ICAENS 2023, July 10 - 12, 2023)

**ATIF/REFERENCE:** Bouhental, B., Hedef, A., Aouachria, Z. & Mameri, A. (2023). The Production of NO/NO<sub>2</sub> Emissions In Propane-Syngas Mixture Diffusion Flame. *International Journal of Advanced Natural Sciences and Engineering Researches*, 7(6), 335-341.

**Abstract** – The increase in energy demand worldwide led to the excessive use of fossil fuels, thus, critical changes in the earth's climate due to its high emissions, which led to the search and the use of less polluting fuels and more sustainable such as Propane and Bio-Syngas. We have used the Chemkine code fed by the USC ver 2.0 mechanism and the Gri Mech 2.11 N sub mechanism for NO<sub>x</sub> assessment to conduct a numerical study on the flame structure and NO<sub>x</sub> emissions characterisation of the Propane-syngas mixture diffusion flame. It was found that rich-Syngase mixtures flames generate high flame temperatures, thus high NO emissions. In contrast, rich-Propane mixture flames generate low flame temperatures, thus high NO<sub>2</sub> emissions.

*Keywords* –

### I. INTRODUCTION

The earth's climate has witnessed lately several critical changes that threaten the lives of its creatures. One of the main changes is the increase in the earth's temperature [1] due to the effect of global warming caused by greenhouse gases, such as carbon dioxide; NO<sub>x</sub> emissions also contribute to the greenhouse effect [2] and climate change, exacerbating global warming. In addition, NO<sub>x</sub> emissions contribute to smog formation and ground-level ozone [3], [4]. High ozone concentrations can harm vegetation, damage crops, and negatively affect ecosystems [5]. Moreover, nitrogen oxides are major contributors to acid rain formation [6], which can harm aquatic life and forest ecosystems.

NO<sub>x</sub> emissions are primarily generated by human activities such as industrial processes, transportation [7], and fossil fuel combustion [8]. Addressing NO<sub>x</sub> emissions is crucial for safeguarding both the environment and human health. Implementing a combination of technological advancements in combustion science and less polluted fuels, known as environmentally friendly fuels, can help minimise these emissions and mitigate their detrimental effects.

Environmentally friendly fuels such as bio-syngas, which is primarily a gas mixture of carbon monoxide and hydrogen obtained from the gasification of biomass, the nature of biomass control of the syngas mixture composition has

witness lately an increasing interest due to its features such as its considerable energy density, the sustainability of its production source as well as being suitable for many combustion systems such as gas turbines [9] and Internal combustion engines [10].

In addition, LPG fuel which is mainly composed of propane [11] has proven to be a strategic fuel for many applications due to the advantages that it provides in terms of economic impact; even though the LPG fuel economy is lower than petrol, from 20% to 25% [12] but due to its low cost compared to petrol by 40% to 50% [13] makes it a more cost-effective option. Moreover, in terms of environmental impact, One of the most environmentally friendly conventional fuels is LPG. When compared to diesel, oil, wood, or coal, it creates far less NOx emissions.

In light of the mentioned above, we conducted a numerical investigation of the impact of Oxygen enhanced-combustion, Preheated air combustion and fuel mixture composition on the NOX emissions especially NO and NO<sub>2</sub> produced from syngas-propane diffusion flame.

II. MATERIALS AND METHOD

1) SIMULATION OF THE PROBLEM

The physical model of opposite flow laminar diffusion flame in Ansys Chemkin code was considered. The model consists of two opposite nozzles separated with a distance equal to 1.5 cm Fig. 1. The upper nozzle represents the oxidiser stream which is air. In contrast, the lower one represents the fuel stream which is a mixture of propane and syngas assumed to be composed of hydrogen and carbon monoxide. The effects of fuel mixture composition, oxygen concentration, and air injection temperature are considered. The flame structure is assumed to be uniform in the longitudinal direction (r) and one-dimensional, with properties dependent only on the transverse direction (x). A section perpendicular to the flame (x direction) is produced to characterise the flame structure. The study's operating conditions are listed in Table 1.

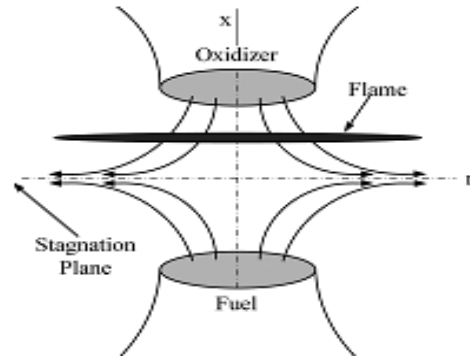


Fig. 1 – Opposed flow geometry in cylindrical coordinates

Table 1 – The operating condition

Fuel	M1	M2	M3	M4
C <sub>3</sub> H <sub>8</sub>	0.4	0.5	0.6	0.7
H <sub>2</sub>	0.3	0.25	0.2	0.15
CO	0.3	0.25	0.2	0.15
T <sub>F</sub> (K)	300			
OXD				
O <sub>2</sub>	0.21			
N <sub>2</sub>	0.79			
T <sub>O</sub> (K)	300			

2) THE GOVERNING EQUATIONS

The governing mathematical equations that describe the combustion phenomenon in the axisymmetric counter-flow configuration is based on the equations of continuity, momentum, species and energy conservation. These equations are proposed by the mathematical model of [14].for the geometry shown in Fig. 1:

The equation of continuity is:

$$\frac{\partial \rho u}{\partial x} + \frac{1}{r} \frac{\partial (\rho v r)}{\partial r} = 0 \tag{1}$$

In Eq. (1), r represents the radial direction, x is the axial direction, u and v are the axial and radial velocity, respectively, and ρ is the mixture density.

The momentum equation writes:

$$H - 2 \frac{d}{dx} \left( \frac{F(x)G(x)}{\rho} \right) + \frac{3G(x)^2}{\rho} + \frac{d}{dx} \left[ \mu \frac{d}{dx} \left( \frac{G(x)}{\rho} \right) \right] = 0 \tag{2}$$

With  $G(x) = \frac{-\rho v}{r}$ ,  $F(x) = \frac{\rho v}{2}$  and  $H = \frac{1}{r} \frac{\partial P}{\partial r} = cste$

The species conservation equation is:

$$\rho u \frac{dY_K}{dx} + \frac{d}{dx} (\rho Y_K V_K) - \dot{\omega}_K M_K = 0; (K = 1, \dots, n) \tag{3}$$

Where the diffusion velocity of the species k is given by:

$$V_K = \frac{1}{X_K} D_{mk} \frac{dX_k}{dx} - \frac{D_k^T}{\rho_k} \frac{1}{T} \frac{dT}{dx} \quad \text{Such as:}$$

$$D_{mk} = \frac{1 - Y_k}{\sum_{j \neq k} \frac{X_j}{D_{jk}}}$$

With  $D_{jk}$ ,  $D_{mk}$  and  $D_k^T$  are, respectively, the diffusion coefficients of the multi-composition, the mean mixture, and the thermal diffusion coefficients of species k.

The energy conservation equation

$$\rho u \frac{dT}{dx} - \frac{1}{C_p} \frac{d}{dx} \left( \lambda \frac{dT}{dx} \right) + \frac{\rho}{C_p} \sum_k C_{pk} Y_k V_k \frac{dT}{dx} + \frac{1}{C_p} \sum_k h_k \dot{\omega}_K + \frac{1}{C_p} \dot{Q}_{rad} = 0 \tag{4}$$

These equations involve various parameters, where  $C_p$  represents the mixture's specific heat capacity,  $h_k$  is the molar enthalpy of species k,  $W_k$  represents the molar mass of species k, and  $\dot{\omega}_K$  represents the chemical production rate of species k.

It would be very useful to characterize NOx emission using the NOx emission index so it would be possible to compare with other flames, it is defined by [15]:

$$EINOx = \frac{\int_0^d W_{NOx} \dot{\omega}_{NOx} dx}{-\int_0^d W_{fuel} \dot{\omega}_{fuel} dx} \tag{5}$$

Both the fuel and the oxidizer are injected with the same velocity, extracted from the corresponding strain rate, which is defined by [16]:

$$a = \frac{-(u_{Ox})}{d} + 2 \frac{u_{Fu}}{d} \sqrt{\frac{\rho_{Fu}}{\rho_{Ox}}} = \frac{2(-u_{Ox})}{d} \left[ 1 + \frac{u_{Fu}}{(-u_{Ox})} \sqrt{\frac{T_{Ox} W_{Fu}}{T_{Fu} W_{Ox}}} \right] \tag{6}$$

### III. RESULTS AND DISCUSSION

The paper comprises two sections; in the first section, we will focus on the impact of the fuel and the oxidizer injection velocities. In contrast, the second section will be more on the impact of fuel composition.

#### 1) The impact of the strain rate

In this section, the impact of the fuel composition on the flame temperature, the production of the free radicals H /OH as well as NO and NO<sub>2</sub> emissions, will be examined. Propane mole fraction will be increased from 0.4 in M1 to 0.7 in M4, leading to syngas reduction from 0.6 in M1 to 0.3 in M4. The fuel and oxidizer injection temperature equals 300 k; the pressure is constant and equal to 1atm; the fuel and the oxidizer injection velocity are the same and equal to the strain rate corresponding to the highest flame temperature. The injection velocity will be determined in the next section.

#### 1.1) On peak flame temperature

Figure. 1 represents the impact of the injection velocity representative in the stain rates on the peak flame temperature; the graphs exhibit a peak pattern at an intermediate value of strain rate equal to  $a = 25 \text{ S}^{-1}$  for all mixtures, where the peak flame temperature exhibits a maximum in each mixture 2125 K for M1, 2098 K for M2, 2073 for M3 and 2052 for M4. Before the intermediate value of strain rate, the peak flame temperature increase with the strain rate as a result of the decrease in the residence time of the radioactive species in the reaction zone, which will inhibit energy losses due to flame radiation, thus, higher flame temperature. However, after that, the impact of radiation is no longer critical, and the combustion reactions will not have the necessary time to be completed due to the continuous decrease in the residence time with the stain rate increase, thus a decrease in the peak flame temperature.

In order to examine the impact of the fuel composition on flame structure and its NOx emission, the strain rate will be fixed at the value corresponding to the highest flame temperature  $a = 25 \text{ S}^{-1}$ .

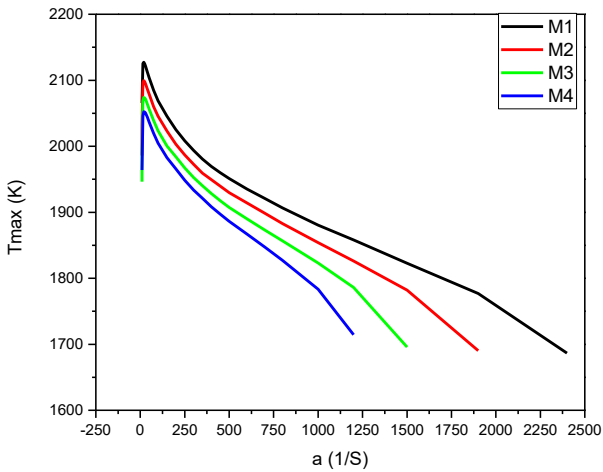


Fig. 1 - Maximum flame temperature in different fuel mixtures as a function of scalar dissipation rate

2) The impact of the fuel composition

2.1) On the temperature distribution

Figure.2 represents the temperature distribution in each mixture in the function of the distance between the nozzles; the temperature increases in M1, M2, M3, then M4, respectively, due to the fact that rich syngas fuel mixture contains more hydrogen, which is more diffusive and reactive. The temperature keeps increasing until it reaches its peak at the flame front where  $T(M1) = 2125$  K at  $x = 0.88$  cm,  $T(M2) = 2098$  K at  $x = 0.89$  cm,  $T(M3) = 2073$  K at  $x = 0.9$  cm and  $T(M4) = 2052$  K at  $x = 0.91$  cm, we note that the flame temperature levels decreased with propane enrichment from M1 to M4 even though that the power input is increased, however after the flame front we note the opposite results the temperature levels increased with propane enrichment from M1 to M4, such finding could be explained by the fact that more propane rich mixture more oxygen it needs to be completed burn, due the lack of oxygen on the fuel side leads to incomplete combustion thus fewer temperature levels, In contrast on the oxidizer side more oxygen will be available thus more complete combustion process and higher temperature levels.

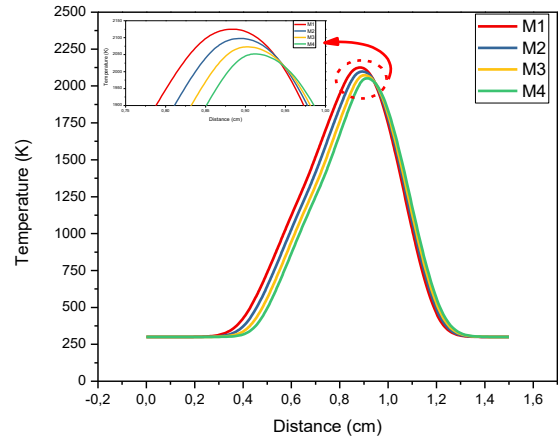


Fig. 2 – Temperature distribution

2.2) On the production of H and OH radicals

Figure.3 represents the production and the distribution of the radical H -a- and the radical OH -b- in each flame, we note that the behaviour of the radicals is similar to the temperature; both radical's mole fractions start increasing in syngas-rich flames first till they reach their maximum at the flame front where for the radical H  $X_{max}(M1) = 3.8E-03$  at  $x = 0.88$  cm,  $X_{max}(M2) = 3.6E-03$  at  $x = 0.9$  cm,  $X_{max}(M3) = 3.4E-03$  at  $x = 0.91$  cm and  $X_{max}(M4) = 3.2E-03$  at  $x = 0.93$  cm, while for the radicals OH  $X_{max}(M1) = 8.7E-03$  at  $x = 0.93$  cm,  $X_{max}(M2) = 8.2E-03$  at  $x = 0.94$  cm,  $X_{max}(M3) = 7.7E-03$  at  $x = 0.95$  cm and  $X_{max}(M4) = 7.7E-03$  at  $x = 0.96$  cm. After that, at the oxidizer side, we note that the radicals mole fraction is higher in propane-rich flames, which also supports our claim before on the temperature distribution because, as known, radicals are very reactive species, so their abundance will result in higher flame temperature levels, it is also worth mention, that the position of the production of OH radicals is just after the position of the H radicals, which point to that the OH resulted from the oxidation of the radical H.

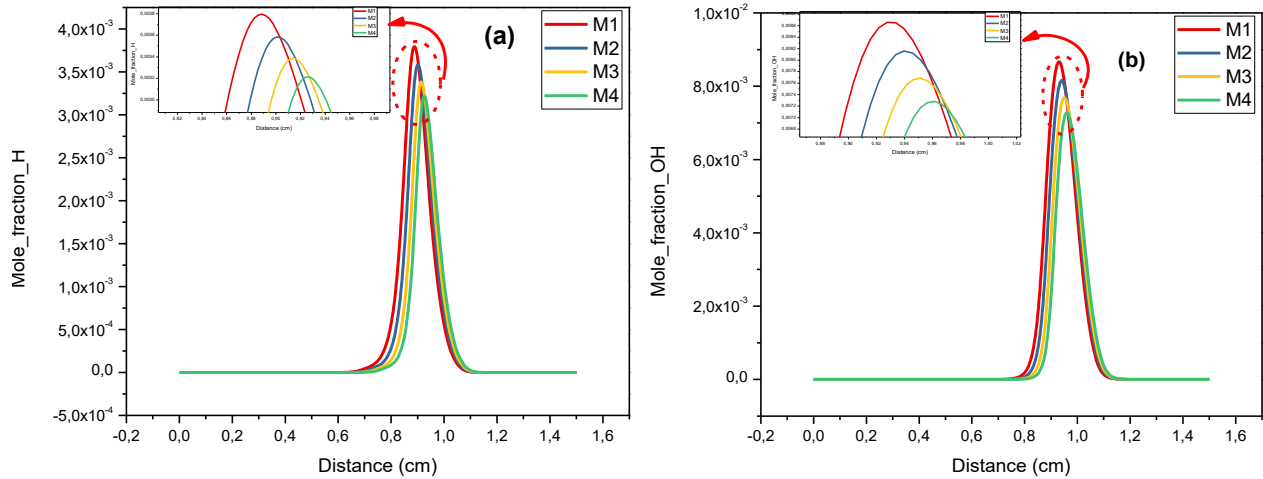
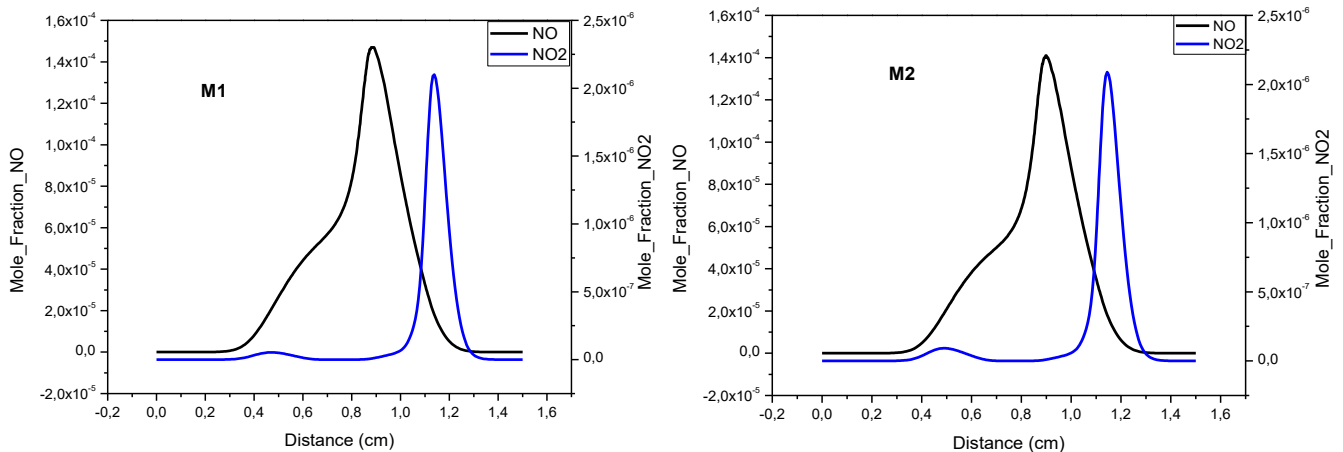


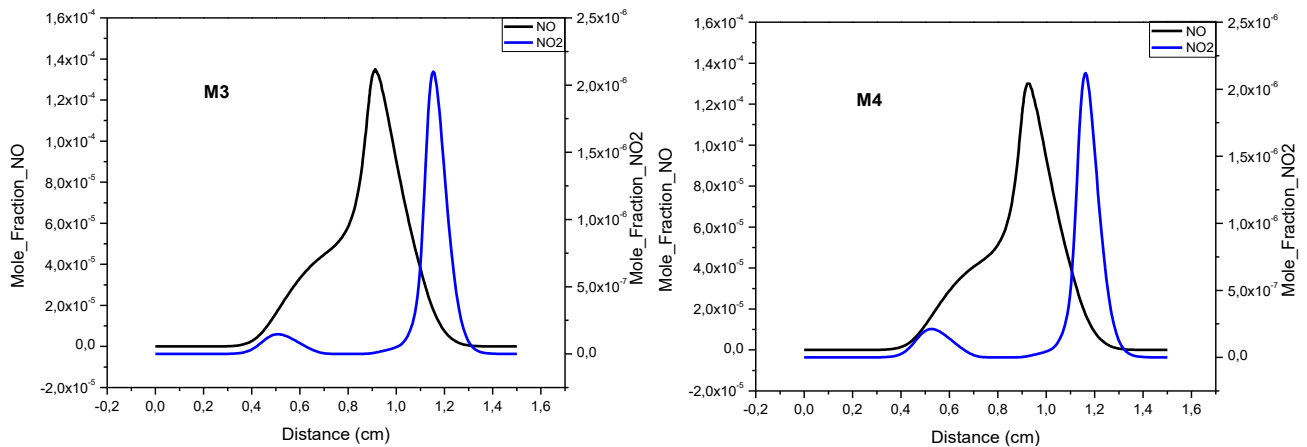
Fig. 3 – The production of the radicals H (a) and OH (b) in each flame

2.3) On the production and the distribution of NO and NO<sub>2</sub> emissions

Figure.5 represents the production and the distribution of NO and NO<sub>2</sub> emissions in each flame in terms of the distance between the nozzles. We note that the production of NO started first at the same position in which the temperature started in increasing; after that, the NO<sub>2</sub> mole fraction increased as well, indicating that NO<sub>2</sub> is a result of NO oxidation. Both NO and NO<sub>2</sub> mole fraction keeps increasing towards the oxidizer side till the NO<sub>2</sub> mole fraction exhibits its first peak in the fuel side  $X(M1) = 5.35E-8$  at  $x = 0.47$  cm,  $X(M2) = 9.16E-8$  at  $x = 0.49$  cm,  $X(M3) = 1.46E-7$  at  $x = 0.51$  cm and  $X(M4) = 2.12E-7$  at  $x = 0.52$  cm than NO<sub>2</sub> decreases to almost zero while NO mole fraction keeps increasing till exhibits a peak at the position of the flame front where  $X(M1) = 1.47E-4$  at  $x = 0.88$  cm,  $X(M2) = 1.41E-4$  at  $x = 0.9$  cm,  $X(M3) = 1.35E-4$  at  $x = 0.91$  cm and

$X(M4) = 1.3E-4$  at  $x = 0.92$  cm than after the flame front on the oxidizer side it starts in decreasing; however NO<sub>2</sub> mole fraction start in increasing again till it exhibits its highest peak on the oxidizer side where  $X(M1) = 2.1E-6$  at  $x = 1.14$  cm,  $X(M2) = 2.09E-6$  at  $x = 1.14$  cm,  $X(M3) = 2.1E-6$  at  $x = 1.16$  cm and  $X(M4) = 2.12E-6$  at  $x = 1.16$  cm. Overall we note that at the same flame, NO production is at a high-temperature region (flame front); this would be attributed to NO production through the thermal route reactions, which its rate of production is directly proportional to the temperature, in addition to NO production through NO<sub>2</sub>-intermediate route which explains the decrease in NO<sub>2</sub> mole fraction first peak. In contrast, NO<sub>2</sub> production is at a low-temperature region due to the oxidation of NO to NO<sub>2</sub>. The availability of nitrogen and Oxygen on the oxidizer side explains why the NO<sub>2</sub> mole fraction second peak is much more significant than the first NO<sub>2</sub> mole fraction first peak.



Fig. 4 – NO/NO<sub>2</sub> species production in each flame

#### IV. CONCLUSION

We have conducted a numerical investigation on the flame structure and NO<sub>x</sub> emissions characterization of Propane-syngas mixture diffusion flame using Chemkine code fed by USC ver 2.0 mechanism coupled with Gri Mech 2.11 N sub mechanism for NO<sub>x</sub> evaluation. The main findings are:

- The flame temperature levels of each flame exhibit a maximum at a value of strain rate at which the heat losses due to flame radiation are no longer important.
- Propane-rich flames need a high amount of oxygen for a more complete combustion process compared to syngas-rich flames.
- Even though its low power input syngas-rich flames generates higher temperature levels than Propane-rich flames.
- NO emission production is favourable in high-temperature regions, while NO<sub>2</sub> emission is favourable in low-temperature regions.

#### REFERENCES

- [1] R. Rohde, R. Muller, R. Jacobsen, E. Muller, S. Perlmutter, A. Rosenfeld, *et al.*, "A new estimate of the average Earth surface land temperature spanning 1753 to 2011. Geoinfor Geostat: An Overview 1: 1," 2013.
- [2] G. Lammel and H. Graßl, "Greenhouse effect of NO<sub>x</sub>," *Environmental Science and Pollution Research*, vol. 2, pp. 40-45, 1995.
- [3] M. I. Khoder, "Diurnal, seasonal and weekdays-weekends variations of ground level ozone concentrations in an urban area in greater Cairo," *Environmental Monitoring and Assessment*, vol. 149, pp. 349-362, 2009.
- [4] D. A. Dam and T. K. O. Nguyen, "Photochemical smog introduction and episode selection for the ground-level ozone in Hanoi, Vietnam," *VNU Journal of Science: Earth and Environmental Sciences*, vol. 24, 2008.
- [5] B. S. Felzer, T. Cronin, J. M. Reilly, J. M. Melillo, and X. Wang, "Impacts of ozone on trees and crops," *Comptes Rendus Geoscience*, vol. 339, pp. 784-798, 2007.
- [6] S. Dubey, "Acid rain-the major cause of pollution: its causes, effects and solution," *International Journal of Scientific Engineering and Technology*, vol. 2, pp. 772-775, 2013.
- [7] J. N. Galloway and E. B. Cowling, "Reactive nitrogen and the world: 200 years of change," *AMBIO: A Journal of the Human Environment*, vol. 31, pp. 64-71, 2002.
- [8] R. Wadanambi, L. Wandana, K. Chathumini, N. Dassanayake, D. Preethika, and U. Arachchige, "The effects of industrialization on climate change," *J. Res. Technol. Eng.*, vol. 1, pp. 86-94, 2020.
- [9] P. Gobatto, M. Masi, A. Toffolo, and A. Lazzaretto, "Numerical simulation of a hydrogen fuelled gas turbine combustor," *International journal of hydrogen energy*, vol. 36, pp. 7993-8002, 2011.
- [10] M. Fiore, V. Magi, and A. Viggiano, "Internal combustion engines powered by syngas: A review," *Applied Energy*, vol. 276, p. 115415, 2020.
- [11] K. J. Morganti, T. M. Foong, M. J. Brear, G. da Silva, Y. Yang, and F. L. Dryer, "The research and motor octane numbers of liquefied petroleum gas (LPG)," *Fuel*, vol. 108, pp. 797-811, 2013.
- [12] (August 23, 2021). *Benefits Of LPG vs Petrol Vehicles*. Available: <https://www.sustainablebusiness toolkit.com/lpg-vs-petrol-vehicles/>

- [13] S. Gupta, "Environmental & economic benefits of Auto LPG as a viable alternative fuel: From cleaner emissions to lower costs," in *Times of India*, ed, March 4, 2022.
- [14] R. J. Kee, J. A. Miller, G. H. Evans, and G. Dixon-Lewis, "A computational model of the structure and extinction of strained, opposed flow, premixed methane-air flames," in *Symposium (International) on Combustion*, 1989, pp. 1479-1494.
- [15] T. Takeno and M. Nishioka, "Species conservation and emission indices for flames described by similarity solutions," *Combustion and flame*, vol. 92, pp. 465-468, 1993.
- [16] H. Chelliah, C. K. Law, T. Ueda, M. Smooke, and F. Williams, "An experimental and theoretical investigation of the dilution, pressure and flow-field effects on the extinction condition of methane-air-nitrogen diffusion flames," in *Symposium (International) on Combustion*, 1991, pp. 503-511.